Solar-Terrestrial Physics. 2025. Vol. 11. Iss.1. P. 81–89. DOI: 10.12737/stp-111202510. © 2025 A.M. Uralov, S.V. Lesovoi, V.V. Grechnev, M.V. Globa. Published by INFRA-M Academic Publishing House

DOI: 10.12737/stp-111202510

Received August 15, 2024
Accepted December 11, 2024

FEATURES OF CORRELATION CURVES OF THE SIBERIAN RADIOHELIOGRAPH

A.M. Uralov
Institute of Solar-Terrestrial Physics SB RAS, Irkutsk, Russia, uralov@iszf.irk.ru

S.V. Lesovoi
Institute of Solar-Terrestrial Physics SB RAS, Irkutsk, Russia, svlesovoi@gmail.com

V.V. Grechnev
Institute of Solar-Terrestrial Physics SB RAS, Irkutsk, Russia, grechnev@iszf.irk.ru

M.V. Globa
Institute of Solar-Terrestrial Physics SB RAS, Irkutsk, Russia, globa@iszf.irk.ru

Abstract. Correlation curves of the multi-frequency Siberian Radioheliograph (SRH) provide a sensitive indication and demonstrative representation of monitoring the microwave life of the active Sun. We derive approximate relationships and briefly discuss the contribution of the quiet Sun, active regions, radio bursts, satellites, and atmospheric absorption to the radioheliograph's correlation response. The estimates are obtained under the assumption that the activity centers and the quiet Sun are homogeneous disks of different sizes and brightness. The sensitivity of the correlation curves to weak sources of small angular sizes is due to their wide spatial spectrum. The wide spectrum means that each pair of antennas produces a noticeable interferometric response, so the total response is significant. The correlation curves allow us to estimate spatial sizes of the radio burst source at different frequencies, but do not allow us to calculate the shape of its radio spectrum. Variability in the atmospheric water content over time creates fluctuations of the received solar radio flux. The correlation response is much less susceptible to this factor.

Keywords: Sun, microwave emission, radioheliograph, correlations.

INTRODUCTION

At the end of 2023, The Siberian Radioheliograph (SRH) was fully commissioned. SRH consists of three multi-element interferometers recording solar microwave emission [Altyntsev et al., 2020]. One interferometer operates in the 3–6 GHz range; the second, in the 6–12 GHz range; the third, in the 12–24 GHz range. Each interferometer performs parallel aperture synthesis (Fourier synthesis) of solar radio images at 16 frequencies, providing a pair of solar images at each frequency with an interval of 3.5 s: one in total intensity (Stokes *I*) and the other in circular polarization (Stokes *V*).

The potential information flow from SRH is so large that the selection of intervals for the analysis of solar activity events (or, conversely, quiet periods) is unlikely to be feasible without a simple time series of a parameter characterizing the intensity of solar radio emission. The generally accepted quantitative characteristic of solar activity is the total flux of soft X-ray emission recorded by the American GOES satellites and presented in real time on the website [https://www.swpc.noaa.gov/]. However, with a general direct statistical relationship between the intensities of soft X-ray emission of a solar flare and the associated microwave burst, a weaker microwave burst may correspond to a stronger soft X-ray emission and vice versa [Fleishman et al., 2011]. Moreover, it is impossible to assess the current state of the radioheliograph based on soft X-ray data. We, therefore, need a parameter formed from the SRH data.

The most obvious characteristic of the solar microwave emission is its total flux obtained by summing signals from all SRH antenna elements. Another characteristic is the SRH correlation response derived by summing the correlation responses of various pairs of its antennas. The time evolution of the SRH correlation response is represented by a correlation curve. Correlation plots were used at the Japanese Nobeyama Radioheliograph (NoRH [Nakajima et al., 1994]), which operated from 1992 to 2020. In the case of NoRH, sufficiently long baselines (8- and 16-fold fundamental spacing, i.e. the minimum distance between antennas) were employed to form the correlation curves; therefore, the corresponding plots were practically free from the contribution of the quiet solar disk, responding to intensity variations only of sufficiently bright and compact sources.

As shown in [Lesovoi, Kobets, 2017], the formation of correlation curves with all possible pairs of radioheliograph antennas allows achieving a sensitivity many times higher than the sensitivity achieved using the total flux. In this case, the contribution to the correlation curve of emission from radio sources of almost all spatial scales and intensities, including the quiet solar disk and extremely weak radio bursts, becomes significant. As such, correlation curves are perceived as microwave indicators of solar activity that are clearer and more sensitive than the total-flux plots. On the one hand, this is indeed the case, which can be easily verified by browsing the website [https://badary.iszf.irk.ru/], where these curves are presented in real time. On the other hand, the everyday use of correlation curves in monitoring and preliminary analysis of the spectral and temporal characteristics of the microwave Sun requires experience and caution. This article is aimed at familiarizing the average user with the simplest features of the SRH correlation curves and is a useful supplement to the articles [Lesovoi, Kobets, 2017, 2018] that contain the formulation and modeling of SRH correlation curves. The monographs [Zheleznyakov, 1970; Thompson et al., 2003] have been chosen as a source of the basic information on radio astronomy we use.

1. FORMATION OF SRH CORRELATION RESPONSE

1.1. Reference information

The radioheliograph response is a combination of N pairs of responses of parabolic antennas. The number of these pairs $N=n(n-1)/2$ when using n antennas. The feed of each antenna is a converter of the electric-field induction E of the electromagnetic wave collected by the antenna mirror into electric current or voltage V. These quantities are proportional to each other, but, omitting the dimensional coefficients of such a conversion, we will put an equal sign between them. In the two-dimensional case for a pair of identical antennas 1 and 2 and a flat front of a uniform-intensity wave incident on both antennas $V_1=E\cos(\omega t)$, $V_2=E\cos(\omega t+\varphi)$, where φ is the phase shift for a point source equal to $\varphi=2\pi B\sin\theta_0/\lambda$. Here B is the distance between the antennas (base); $\theta_0=\theta_0(t)$ is the zenith distance expressed in radians; ω is the angular frequency of the received radio emission; λ is its wavelength.

In radio astronomy, the density of the electromagnetic energy flux is usually used which is a quantity proportional to the time-averaged square of the electric-field induction of a radio wave. Formal addition of electric signals from two antennas, squaring and averaging over time (angle brackets) yield the well-known result of their interference

$$R=\left\langle \left(V_1+V_2\right)^2\right\rangle=\left\langle V_1^2\right\rangle+\left\langle V_2^2\right\rangle+2\left\langle V_1V_2\right\rangle= \\ =E^2/2+E^2/2+E^2\cos\varphi. \qquad (1)$$

The terms $\left\langle V_{1,2}^2\right\rangle=E^2/2$ are proportional to the emission fluxes F collected by each of the antennas and having the dimension of power. Replacing the proportionality of these quantities with their equality means $E^2/2=F$. The interference multiplier $\left\langle V_1V_2\right\rangle$, which is the time average of the product of antenna signals, characterizes their covariance and is the subject of further interest. Devices operating on the basis of additive relation (1) are an optical diffraction grating with a lens or an array of antennas connected by waveguides whose combination plays the role of a lens. Such was the Siberian Solar Radio Telescope that performed sequential aperture synthesis. The operating principle of SRH as parallel aperture synthesis is different which does not require direct summation of electric signals of the antennas. Nonetheless, when moving from a point radio source to an extended one and to a multi-element interferometer, we leave relation (1). It contains all the information necessary to construct the total-flux plots, radio images of the active Sun, and their relationship in the form of correlation curves presented on the website [https://badary.iszf.irk.ru/].

An extended source is considered as a mosaic of small (point) elements with the index j. The expression for the phase shift on the ith antenna pair from each such element is rewritten as

$$\varphi_{ij}=2\pi B_i\sin\left(\theta_0+\Delta\theta_j\right)/\lambda=\left(2\pi B_i/\lambda\right)\times \\ \times\left(\sin\theta_0\cos\Delta\theta_j+\cos\theta_0\sin\Delta\theta_j\right). \qquad (2)$$

Here $\theta_0=\theta_0(t)$ is the zenith distance of the selected center of a radio source moving across the sky (in our case, such a center is assumed to be the solar disk center whose position is being calculated); $\Delta\theta_j$ is the angular distance of the jth element of the mosaic from the center of the radio source. Introducing the notation $\varphi_0=2\pi B_i\sin\theta_0/\lambda$, $\Delta\varphi_{ij}=\varphi_{ij}-\varphi_0$ and using the expansion in $\Delta\theta_j\ll 1$ accurate to linear terms, we find $\Delta\varphi_{ij}=(2\pi B_i\cos_0/\lambda)\Delta\theta_j$. The product $B_i\cos\theta_0$ is the base of the antenna pair visible from the radio source center. Relation (2) with only one direction angle fits the educational flat picture, where the antenna pair, the zenith point, and the radio source lie in the same plane.

The generalization of relation (2) to the three-dimensional case in vector form is as follows:

$$\varphi_{ij}=2\pi\left(\vec{B}_i\,\vec{\theta}_j\right)/\lambda=\varphi_0+\Delta\varphi_{ij},\ \vec{\theta}_j=\vec{\theta}_0+\overrightarrow{\Delta\theta}_j, \\ \varphi_0=2\pi\left(\vec{B}_i\,\vec{\theta}_0\right)/\lambda,\ \Delta\varphi_{ij}=2\pi\left(\vec{B}_i\,\overrightarrow{\Delta\theta}_j\right)/\lambda. \qquad (3)$$

Here $\vec{\theta}_0$ and $\vec{\theta}_j$ are unit vectors of directions to the source center and its small element with the j index; $\overrightarrow{\Delta\theta}_j$ is the angular distance between these directions; $\vec{B}_i$ is the vector of the base of the ith antenna pair.

When observing an extended object, formal relation (1) valid for a point source is replaced by a similar relation for the ith antenna pair

$$R_i=\left\langle\left(\sum_j V_1^j+\sum_{j'} V_2^{j'}\right)^2\right\rangle= \\ =\left\langle\sum_j\left(V_1^j\right)^2\right\rangle+\left\langle\sum_j\left(V_2^j\right)^2\right\rangle+2\left\langle\sum_j\left(V_1^jV_2^j\right)\right\rangle= \\ =2\sum_j\frac{1}{2}E_j^2+\sum_j E_j^2\cos\varphi_{ij}=2F+2r_i. \qquad (4)$$

Here $F=\sum_j\frac{1}{2}E_j^2$ is the total flux received by one antenna; $r_i=\left\langle V_1V_2\right\rangle=\left\langle\sum_j\left(V_1^jV_2^j\right)\right\rangle=\sum_j\frac{1}{2}E_j^2\cos\varphi_{ij}$ is the interferometric response or covariance obtained for each antenna pair by a device called a correlator. In expression (4), all terms of the form $\left\langle V_*^jV_*^{j'}\right\rangle$, where asterisks denote combinations of 1 and 2, are omitted. Such terms vanish for $j \neq j'$ (otherwise, the problem of aperture synthesis is unsolvable). Such a representation of the response of the *i*th antenna pair to the emission flux of an extended object is possible only under the assumption that all elementary *j* sources are mutually incoherent. The assumption of mutual incoherence corresponds to reality. A set of independent solar radio sources can operate as a single coherent source when they are all located inside the size of the first Fresnel zone $a_{\mathrm{Fr}} \simeq \sqrt{z\lambda}$, if viewed from a vantage point located at a distance *z* from the Sun. The size of a_{Fr} can be considered the physical definition of a point source. For an observation frequency of 10 GHz, $a_{\mathrm{Fr}}\simeq70$ km, i.e. $\simeq0.1''$, which is two orders of magnitude less than the angular resolution achievable at SRH. Such a limiting resolution is hypothetically achievable with interferometer sizes comparable to a_{Fr}, but in this case for its longest baseline the approximation of the far wave field used in aperture synthesis would be violated because the conditional boundary between the near and far wave field zones reaches the Sun.

The transition in expressions (4) for *F* and r_i from summation over discretely arranged *j* elements to continuous integration over all directions $\vec{\theta}$ leads to the disappearance of the *j* index in relations (3): $\vec{\theta}_j \to \vec{\theta}$, $\varphi_{ij} \to \varphi_i$. For an extended object, the values of *F* and r_i are now determined by the formulas

$$
\begin{aligned}
F &= \Delta\nu A\int_\Omega D\left(\nu,\vec{\theta}\right) I\left(\nu,\vec{\theta}\right) d\Omega \\
r_i &= \Delta\nu A\int_\Omega D\left(\nu,\vec{\theta}\right) I\left(\nu,\vec{\theta}\right) \cos\varphi_i \, d\Omega.
\end{aligned}
\tag{5}
$$

Here $d\Omega$ is the element of the solid angle over which the integration is performed; $I\left(\nu,\vec{\theta}\right) = \dfrac{k}{\lambda^2} T_{\mathrm{b}}\left(\nu,\vec{\theta}\right)$ is the angular distribution of incident-emission intensity [W/(m^2·Hz·sr)] for one circular-polarization mode; $T_{\mathrm{b}}\left(\nu,\vec{\theta}\right)$ is the angular brightness-temperature distribution corresponding to this mode; $D\left(\nu,\vec{\theta}\right)$ is the power beam pattern of a single antenna (the antenna follows the source as it moves across the sky); *k* is the Boltzmann constant; *A* is the effective area of the antenna; $\Delta\nu$ is the frequency band of the receiving channel. The upper integral in (5) is the spectral density of the emission flux received by a single antenna. Substituting relations (3) in (5) (dropping the *j* index) yields

$$
\begin{aligned}
r_i &= \Delta\nu A\int_\Omega D\left(\nu,\vec{\theta}\right) I\left(\nu,\vec{\theta}\right) \cos\left(\varphi_0 + \Delta\varphi_i\right) d\Omega = \\
&= a_i \cos\varphi_0 + b_i \sin\varphi_0 = \sqrt{a_i^2 + b_i^2}\cos\left(\varphi_0 + \psi_i\right), \\
\psi_i &= \arctan\left(b_i / a_i\right); \\
a_i &= \Delta\nu A\int_\Omega D\left(\nu,\vec{\theta}\right) I\left(\nu,\vec{\theta}\right) \cos\Delta\varphi_i \, d\Omega, \\
b_i &= -\Delta\nu A\int_\Omega D\left(\nu,\vec{\theta}\right) I\left(\nu,\vec{\theta}\right) \sin\Delta\varphi_i \, d\Omega.
\end{aligned}
\tag{6}
$$

In radio interferometry, expression (3) for the additional phase shift $\Delta\varphi_i = 2\pi\left(\vec{B}_i\,\overrightarrow{\Delta\theta}\right)/\lambda$ is written in a local coordinate system tied to the center of the radio source θ_0. In this system, $\Delta\varphi_i$ is equivalent to φ_{ij} (3) for θ_0=0. Then, under the condition $\sin\Delta\theta \approx \Delta\theta$ and in the generally accepted notation

$$
\begin{aligned}
\Delta\varphi_i &= \left(\vec{\kappa}_i\,\overrightarrow{\Delta\theta}\right) = 2\pi\left(u_i l + \upsilon_i m\right), \\
\vec{\kappa}_i &= 2\pi\vec{B}_i/\lambda = 2\pi\left(\vec{u}_i + \vec{\upsilon}_i\right), \\
\kappa_i &= 2\pi\sqrt{u_i^2 + \upsilon_i^2}\,.
\end{aligned}
$$

Here *l*, *m* are angles in radians measured from the center of the source along the directions $\vec{u}_i$ and $\vec{\upsilon}_i$, where $u_i\lambda$ and $\upsilon_i\lambda$ are the projections of the antenna baseline visible from the source on orthogonal axes, which in our case coincides with the directions of the SRH arms.

In the new notation, relation (6) is written as:

$$
\begin{aligned}
r_i &= r_{\cos} + r_{\sin} = a_i \cos\left(\vec{\kappa}_i\,\vec{\theta}_0\right) + b_i \sin\left(\vec{\kappa}_i\,\vec{\theta}_0\right), \\
a_i &= \Delta\nu A\int_\Omega D\left(\nu,\vec{\theta}\right) I\left(\nu,\vec{\theta}\right) \cos\left(\vec{\kappa}_i\,\overrightarrow{\Delta\theta}\right) d\Omega, \\
b_i &= \Delta\nu A\int_\Omega D\left(\nu,\vec{\theta}\right) I\left(\nu,\vec{\theta}\right) \sin\left(\vec{\kappa}_i\,\overrightarrow{\Delta\theta}\right) d\Omega.
\end{aligned}
\tag{7}
$$

The coefficients *a*, *b* have the form of Fourier coefficients for a spatial harmonic with the wave vector $\vec{\kappa}_i$ in the angular distribution of the function $D\left(\nu,\vec{\theta}\right) I\left(\nu,\vec{\theta}\right)$. This function is close to the true intensity distribution $I\left(\nu,\vec{\theta}\right)$ since the half-power width of the main lobe of the beam pattern of single SRH antennas is 2–4 times greater than the angular diameter of the Sun. With some accuracy, we, therefore, further assume $D\left(\nu,\vec{\theta}\right) = 1$.

Relations (6) and (7) can be rewritten using the complex quantity formalism:

$$
\begin{aligned}
\boldsymbol{r}_i &= \left\langle V_1 V_2^* \right\rangle = r_{\cos} + \boldsymbol{i} r_{\sin} = \\
&= a_i \cos\left(\vec{\kappa}_i\vec{\theta}_0\right) + \boldsymbol{i} b_i \sin\left(\vec{\kappa}_i\vec{\theta}_0\right).
\end{aligned}
$$

In this case, the interferometric response $\boldsymbol{r}_i$ is called the complex visibility function or the complex visibility of an extended radio source of a given antenna pair. The visibility function magnitude $\sqrt{a_i^2 + b_i^2}$ has the dimension of the emission flux and is equal to the amplitude of the spectral harmonic $\cos\left(\vec{\kappa}_i\vec{\theta}_0 + \psi_i\right)$ in the angular distribution of the intensity of a radio source the position of whose center moves across the sky along with the vector $\vec{\theta}_0$.

Ideally, the set of complex visibilities of all the SRH antenna pairs is an image of a celestial radio source in intensity. The instantaneous integral characteristic of the spatial spectrum and brightness of this image is the point of the SRH correlation curve $C(t)$. However, when computing the SRH correlation curves, not the visibilities per se are used, but the magnitudes of related quantities, i.e. complex correlation coefficients of signals C_i received by each ith antenna pair. The correlation coefficient is convenient because it is dimensionless and by definition is equal to $C_i = \langle V_1 V_2^* \rangle / \sqrt{\langle V_1^2 \rangle \langle V_2^2 \rangle} = \boldsymbol{r}_i / F_i$. The last relation is a consequence of the idealization we use $\langle V_1^2 \rangle = \langle V_2^2 \rangle = F_i$, where F_i is the emission flux received by a separate antenna. The antenna elements and the accuracy of their pointing to the Sun are also assumed to be identical, and the value of F_i=F to be the same.

Thus, the SRH correlation curve is the time dependence of the sum of the magnitudes of the correlation coefficients C_i of all antenna pairs

$$C(t,\nu) = \frac{1}{N}\sum_i^N \left|C_i(t,\nu)\right| = \frac{1}{N}\sum_i^N \frac{|\boldsymbol{r}_i|}{F_i} = \frac{1}{NF}\sum_i^N \sqrt{a_i^2 + b_i^2}. \quad (8)$$

In other words, $C(t, \nu)$ is the normalized sum of amplitudes (visibilities $|\boldsymbol{r}_i|$) of N spatial harmonics of the spectral series. On the plane of the sky perpendicular to the line of sight, this series corresponds to a two-dimensional periodic sequence of solar images in the main maxima of the SRH diffraction pattern spaced from each other by angles not exceeding $\left(u_{\min}^{-1}; \upsilon_{\min}^{-1}\right)$ radians.

1.2. Sensitivity of correlation curves to weak events

The sensitivity of the correlation curves $C(t, \nu)$ to weak events should not be confused with the sensitivity of the radioheliograph to the received emission flux. The difference between these characteristics can be seen in the example of two sources whose emission fluxes are equal, whereas their angular sizes differ considerably. The correlation response of the radioheliograph to emission from a small source is considerably higher than the response to a large source. Conversely, the correlation responses to both sources may be comparable when the emission flux from a small source is much lower than the emission flux from a large source. It is in this sense that the sensitivity of the correlation curves should be understood.

This sensitivity to weak events of small angular sizes is determined by their visibilities in (8) and can be simply illustrated by the example of a hypothetical point-like radio source the electromagnetic wave from which can be considered plane on the heliograph scale. In this case, $C(t, \nu)$=$C_i(t, \nu)$=1 and the sum $\sum_i^N |\boldsymbol{r}_i|$ of the visibility magnitudes is directly proportional to the number of antenna pairs of the interferometer and is equal to $FN = \frac{n-1}{2} Fn.$ With an increase in the number of antennas and for $n-1 \gg 1$ the sensitivity of the correlation curves $C(t, \nu)$ to weak compact radio sources increases as Fn^2, i.e. much faster than the emission flux Fn received by all interferometer antennas. This circumstance reproduces the well-known property of an equidistant diffraction grating consisting of n slits: the angular redistribution of the electromagnetic field of a plane wave that has passed through the grating is such that at the diffraction maxima the intensity of the wave is n^2 times higher than the intensity from a single slit [Yavorsky, Detlaff, 1965].

Thus, the sensitivity of the correlation curves to weak sources of small angular sizes $\delta\theta$ is due to their wide spatial spectrum $\Delta\kappa \sim 1/(\delta\theta)$. The interval $\Delta\kappa$ contains almost the entire set of wave numbers κ_i of spectral harmonics, each corresponding to the ith antenna pair. This ensures the occurrence of a noticeable interferometric response for each antenna pair of the radioheliograph. A set of N responses forms a total signal.

1.3. Estimated correlation values

The values of correlation curve (8) are determined by the coefficients a and b representing the visibilities $r_{\cos}$ and $r_{\sin}$ of each antenna pair in expression (7). It is impossible to estimate the visibility values a priori since they depend not only on the intensity of the quiet-Sun's emission, but also to a large extent on the relative arrangement and sizes of the brightness forms of the radio sources that are present on the solar disk and above the limb. Nevertheless, general estimates can be made by simplifying the real situation. The first simplification involves replacing radio sources of different sizes with disks of uniform intensity $I(\Omega)$=I_{s}. The second simplification is to schematically arrange all such disks in the phase center, which is the solar disk center. In this case, b=0, ψ=0; in expressions (6), (7), only the even cosine component of the visibility function is preserved, and then

$$C(t,\nu) \Rightarrow C_{\cos}(t,\nu) = \frac{1}{NF}\sum_i^N |a_i|. \quad (9)$$

It is useful to note that although $\sum_i^N |a_i|$ and $\sum_i^N \sqrt{a_i^2 + b_i^2}$ have the dimension of energy flux, they do not pretend to be an energy invariant characterizing the total emissivity of the quiet Sun and radio sources located on it. Such an invariant does not depend on the permutation of sources. The invariant is not the sum of the absolute values of amplitudes of all spatial harmonics as in (8) or (9), but the sum of the squares of their amplitudes.

After simplifications (7), the following expression remains for the coefficient a_i of a circular homogeneous source with radius θ_{s}:

$$\begin{aligned} a_i &= \Delta\nu A I_{\mathrm{s}} \int_\Omega \cos\left(\vec{\kappa}_i \overrightarrow{\Delta\theta}\right) d\Omega = \\ &= \Delta\nu A I_{\mathrm{s}} \int_0^{\theta_{\mathrm{s}}} 4\sqrt{\theta_s^2 - (\Delta\theta)^2} \cos(\kappa_i \Delta\theta)\, d(\Delta\theta) = \\ &= F_{\mathrm{s}} \frac{2 J_1(x_i)}{x_i}; \\ x_i &= \kappa_i \theta_s, \kappa_i = 2\pi\sqrt{u_i^2 + \upsilon_i^2}. \end{aligned} \quad (10)$$

The last integral in (10) is tabulated ([Gradshtein, Ryzhik, 1971], p. 433). $F_s=\Delta\nu A I_s \Omega_s$ [W] is the emission flux from a source S received by one antenna; $\Omega_s=\pi\theta^2$ is the solid angle of the source; J_1 is the Bessel function of the first kind. As follows from (10), the visibility of each component of the spatial spectrum of a source is entirely determined only by its size and brightness. The emission flux of the active Sun is composed of the emission fluxes from sources of three spatial scales: the quiet solar disk with radius $\theta_s=\theta_\odot$, $F_s=F_\odot$; "quiet" active regions (ARs), $\theta_s=\theta_{AR}$, $F_s=F_{AR}$; radio bursts angular sizes of whose sources $\theta_s=\theta_{burst}$ are of the order of or noticeably smaller than the angular size θ_{beam} of the SRH beam pattern, $F_s=F_{burst}$. To estimate the values of points on the correlation curve, we rewrite (9):

$$
\begin{aligned}
&C \Rightarrow C_{\cos} = C_\odot + C_{\mathrm{AR}} + C_{\mathrm{burst}},\\
&C_\odot = \frac{F_\odot}{NF}\sum_i^N \left|\frac{2J_1(\kappa_i\theta_\odot)}{\kappa_i\theta_\odot}\right|,\\
&C_{\mathrm{AR}} = \frac{F_{\mathrm{AR}}}{NF}\sum_i^N \left|\frac{2J_1(\kappa_i\theta_{\mathrm{AR}})}{\kappa_i\theta_{\mathrm{AR}}}\right|, \qquad (11)\\
&C_{\mathrm{burst}} = \frac{F_{\mathrm{burst}}}{NF}\sum_i^N \left|\frac{2J_1(\kappa_i\theta_{\mathrm{burst}})}{\kappa_i\theta_{\mathrm{burst}}}\right|,\\
&F = F_\odot + F_{\mathrm{AR}} + F_{\mathrm{burst}}.
\end{aligned}
$$

Before discussing the relative contribution of these sources to the correlation curves, we define the average base from the set of bases $B_i = \lambda\kappa_i/(2\pi) = \lambda\sqrt{u_i^2+\upsilon_i^2}$ as $\overline{B} = \frac{1}{N}\sum_i^N B_i$. Almost all antennas in the arms of the SRH T-shaped interferometers are located equidistantly in steps of $B_{\min}$. In this case, half of N pairs of antenna bases are located in the interferometer arms, the other half are cross bases of the orthogonal arms. Bearing in mind the rough estimate of $\overline{B}$, we replace the T-shaped interferometer with a linear one with a step of $B_{\min}$ and maintaining the total number of antennas n. In this case, the number of equivalent antenna pairs decreases linearly with increasing base from $(n-1)$ with base $B_{\min}$ to 1 with maximum base $B_{\max}=(n-1)B_{\min}$. It is easy to see that in this case for the average base and average wave number $\overline{\kappa}$ the following relations are obtained:

$$
\begin{aligned}
&\overline{B} = \frac{1}{N}\sum_i^N B_i = \frac{n(n^2-1)}{6N}B_{\min} = \frac{(n+1)}{3}B_{\min},\\
&\frac{2\pi}{\overline{\kappa}} = \frac{\lambda}{\overline{B}} \approx \frac{3\lambda}{nB_{\min}}.
\end{aligned} \qquad (12)
$$

For a linear interferometer, the ratio $\frac{\lambda}{(n-1)B_{\min}} \approx \frac{\lambda}{nB_{\min}}$ is equal to the angular size of the beam pattern θ_{beam}. When maintaining the total number of antennas n, an interferometer consisting of two orthogonal linear interferometers has almost twice the value of $\theta_{beam} \approx \frac{\lambda}{(n/2)B_{\min}}$; therefore, returning to the SRH T-shaped geometry, for $\overline{\kappa}$ we have an estimate

$$
\frac{2\pi}{\overline{\kappa}} \approx 6\theta_{beam},\ \overline{\kappa} \approx \frac{1}{\theta_{beam}}. \qquad (13)
$$

These estimates will be useful for a rough assessment of the contribution of the emissions from the quiet Sun and active regions to the correlation curves.

Thus, relations (11) are the basis for the additive estimate of the correlation curves of the active Sun. The activity centers and the quiet Sun are represented by homogeneous disks of different sizes and brightness. Their mutual arrangement is ignored.

1.4. Difference between the spectral index of the emission flux and that measured from the correlation curves

Another remark concerns caution in the preliminary estimation of the spectral index of the emission flux of a source S from correlation curves $C(t, \nu)$. Such temptation is present in the preliminary analysis of the total spectra of weak radio bursts. As can be seen from (11), the value of $C(t, \nu)$ is determined by the product of F_s/F and the interference factor containing the Bessel functions. Both factors depend on the frequency ν. The interference factor does not distort the total spectrum of the emission source only under the condition $\theta_s \propto 1/\nu$, which rather approximately corresponds to reality ($2\theta_s$ is the angular diameter of the radio source). Nonetheless, even if this condition holds, the distortion of the real spectrum is significant. The denominator of the first factor essentially contains the monotonous spectrum of the quiet Sun $F_\odot$, shown in panel *a* of the figure. Panel *b* presents the distribution of the spectral index α in the local fit $F_\odot \propto \nu^\alpha$ of different portions of this spectrum. The F_s spectra of gyroresonance sources above sunspots and gyrosynchrotron sources in bursts differ greatly from $F_\odot$ in these indices.

This is illustrated by the example of a weak radio burst $F_s = F_{burst} \ll F \approx F_\odot$, whose spectrum portion is a power-law function $F_{burst} \propto \nu^\delta$. In this case,

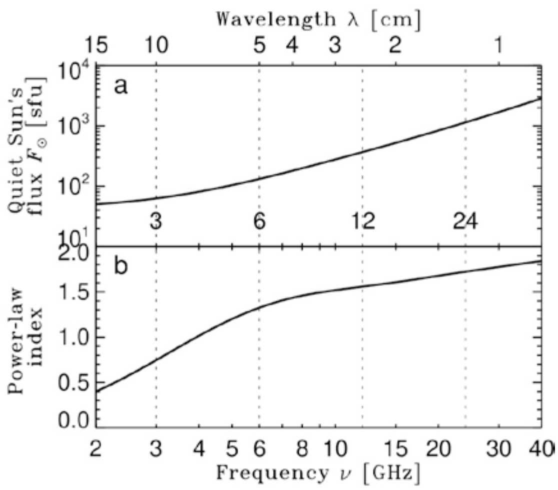

Frequency dependence of the quiet Sun's radio emission flux. We have used observational data from [Borovik, 1994; Zirin et al., 1991]

$C_{\text{burst}}(\nu) \propto F_{\text{burst}}(\nu)/F_\odot(\nu) \propto \nu^{\delta-\alpha}$. The correlation spectral index δ–α obtained from correlation curves differs significantly from the true δ.

Thus, correlation curves allow us to estimate the spectral range of a radio burst, but not the shape of its spectrum.

2. SPECIAL CASES

2.1. Quiet Sun

In this case, F=$F_\odot$ and according to (11)

$$C_{\cos} = C_\odot = \frac{1}{N}\sum_i^N \left| \frac{2J_1(\kappa_i\theta_\odot)}{\kappa_i\theta_\odot} \right|. \quad (14)$$

The use of all components of the spatial spectrum in the calculation of the SRH correlation curves means that the values of the argument $\kappa_i\theta_\odot$ under the summation sign can take values of both <1 and $\gg 1$. This complicates the analysis of expression (14). The spectral components corresponding to the shortest baselines of antenna pairs make the largest individual contribution to $C_\odot$. Yet, the number of such low-frequency components is considerably smaller than the high-frequency ones whose individual contribution is small. The first rough step in the qualitative assessment of “what wins” is the use of relation (13). The determining parameter is the ratio of the angular radius of the Sun $\theta_\odot$ to the wavelength of the average spatial harmonic $2\pi/\bar{\kappa}$, whose angular size is about six times larger than the SRH beam pattern θ_{beam}. The use of relation (13) in this context corresponds to the equality of contributions of all baselines to $C_\odot$, which is valid only for a point source. Nevertheless, due to the condition $\bar{\kappa}\theta_\odot \gg 1$ it is reasonable to use the asymptotic representation of the Bessel function for $\kappa\theta_\odot \gg 1$ in (14). This representation allows us to estimate $C_\odot$ as follows:

$$C_\odot \geq \frac{1}{N}\sum_i^N \left| x_i^{-3/2}\cos\left(x_i + \frac{\pi}{4}\right)\right|, \quad x_i = \kappa_i\theta_\odot. \quad (15)$$

Giving preference not to the accuracy of the numerical value of $C_\odot$, but to the dependence of $C_\odot$ on the wavelength λ of the received radio emission and the SRH angular resolution θ_{beam}, we replace κ_i and $\left|\cos\left(x_i + \frac{\pi}{4}\right)\right|$ in (15) with their average values $\langle \kappa_i \rangle = \bar{\kappa}$ (13) and $\langle |\cos| \rangle = 2/\pi$, which is probably valid only for a large number of antennas:

$$C_\odot \geq \frac{2}{\pi}\left(\bar{\kappa}\theta_\odot\right)^{-3/2} \approx 0.6\left(\frac{\theta_{\text{beam}}}{\theta_\odot}\right)^{3/2} \propto \left(\frac{\lambda}{\bar{B}}\right)^{3/2}. \quad (16)$$

Here we have neglected the dependence of $\theta_\odot$ on λ. The values of $C_\odot$ are determined by the size of the beam pattern θ_{beam}, which changes with the season and during the day according to the position of the Sun. The diurnal variation in θ_{beam} determines the general concavity of the $C(t,\nu) = C_\odot$ plot with a minimum at the noon and its smooth irregularities located symmetrically relative to the noon minimum. The value $C_\odot \propto \nu^{-3/2}$; therefore, the higher the frequency ν, the lower and denser the SRH correlation curves corresponding to the set of equidistant frequencies. Assuming $\theta_\odot = 900''$ in (16) and estimating the minimum values of $\theta_{\text{beam}}(\nu) \approx (3/\nu_{\text{GHz}})32''$, we find $C_\odot(\nu) \geq 4\cdot 10^{-3}(3/\nu_{\text{GHz}})^{3/2}$, $C_\odot(24_{\text{GHz}}) \geq 1.8\cdot 10^{-4}$.

The presence of ARs on the solar disk introduces significant adjustments determined by their angular sizes and the relationship between $F_\odot$ and F_{AR}. This relationship, in turn, reflects the difference between the exponents of the frequency spectra of the microwave emission fluxes of ARs and the quiet Sun. The angular sizes of bright gyroresonance radio sources inside ARs also depend significantly on the frequency, which is not the case in the approximation of a uniform solar disk. These circumstances increase the numerical value and change the mutual arrangement of the correlation curves $C(t, \nu)$.

Thus, relations (15) and (16) give an idea of the magnitude and daily trend of the values of the correlation curves when the Sun is quiet and there are no active regions on it.

2.2. Active regions

Quasi-stationary sources in active regions are responsible for the slowly changing S component of solar radio emission [Zlotnik, 1968]. The microwave emission of AR is determined to the greatest extent by its photospheric magnetogram that is multiscale. Its main spatial size coincides with the characteristic size of plages that exist in the chromosphere and lower corona from the magnetic flux emergence until the disappearance of AR. The radio emission of a plage determines the characteristic size of an AR microwave image in intensity. Within this scale, bright and compact gyroresonance radio sources above sunspots stand out. In intensity, the emission fluxes from the radio plage and sunspot-associated sources can be comparable. The magnitude of the AR visibility function in the simplest situation is therefore determined by the sum of visibilities of sources with two different spatial scales. Nonetheless, we start our consideration by replacing each AR with an effective one of a single spatial scale.

In this case, it follows from expression (11) that C=$C_\odot$+C_{AR}. Formal use of relation (16) with the replacement of $\theta_\odot \Rightarrow \theta_{\text{AR}}$ gives

$$C_{\text{AR}} \geq \frac{F_{\text{AR}}}{F}0.6\left(\frac{\theta_{\text{beam}}}{\theta_{\text{AR}}}\right)^{3/2} = \frac{F_{\text{AR}}}{F_\odot + F_{\text{AR}}}C_\odot\left(\frac{\theta_\odot}{\theta_{\text{AR}}}\right)^{3/2}. \quad (17)$$

This relation is valid for both one AR and for an arbitrary number of ARs, but under the assumption that all

ARs have the same size θ_{AR} and effective brightness temperatures T_b^{AR}. A change in the number of ARs or in T_b^{AR} is automatically taken into account by changing F_{AR}.

In years of active Sun, the total spectral densities of the emission flux from ARs and the quiet Sun are comparable in the SRH frequency range, so for rough estimates we set $F_\odot \approx F_{AR}$. During this period, as observations show, the values of C_{AR} are several times greater than those of $C_\odot$. Assuming $C_{AR}/C_\odot = m \sim 5$, in (17), we obtain a conditional estimate of the size of an effective AR $\theta_{AR}^{eff} \approx (2m)^{-2/3}\theta_\odot \sim \theta_\odot/5$. Active regions of such size exist, but are exceptional. Nevertheless, the inequality $\theta_{AR}^{eff} \gg \theta_{beam}$ justifies the use of the expansion for large arguments of the Bessel function in (11) to estimate at least the radio plage component C_{AR}. The values of θ_{AR}^{eff}, exceeding the typical sizes of developed ARs indicate the need to separately consider the contribution of compact sunspot-associated radio sources to the correlation curve.

Thus, relations (17) present an estimate of the contribution of non-compact $\theta_{AR} \gg \theta_{beam}$ solar active regions to the SRH correlation curves.

2.3. Compact radio source

The interferometric response to a compact radio source is quantitatively close to the response to a point source when for all antenna pairs $x_i = \kappa_i\theta_s \ll 1$ in (10) and $\frac{2J_1(x_i)}{x_i} = 1$. The point source approximation also works well for x_i=1 because in this case $\frac{2J_1(x_i)}{x_i} = 0.88$. Since the maximum wave number of the spatial spectrum corresponds to $\kappa_i \approx 2\pi/\theta_{beam}$, the condition for a point source for all antenna pairs is $2\pi\theta_s \le \theta_{beam}$. There is only one antenna pair with the longest baseline, whereas the number of antenna pairs with the shortest baselines is large, so, when estimating the real contribution of compact sources to the correlation curve, average wave number (13) $\bar{\kappa} \approx 1/\theta_{beam}$ should be used. Then the condition for compactness of the source $\bar{\kappa}\theta_s \le 1$ becomes the well-known and intuitive inequality $\theta_s \le \theta_{beam}$. Under this condition, the contribution of the compact source to the correlation curves is mainly determined by the spectral flux F_s, which, in turn, may be a function of the angular size of the emission source:

$$C_s \approx \frac{F_s}{F}. \tag{18}$$

Thus, relation (18) provides an estimate of the correlation response to a radio source of size $\theta_s \le \theta_{beam}$. The same relation follows with sufficient accuracy from (17) for $\theta_s \simeq \theta_{beam}$, although (17) was obtained under the condition $\theta_s \gg \theta_{beam}$. In this regard, let us note the following circumstance. In a stationary situation, it is practically impossible either to measure F_s or to detect active regions along with compact radio sources, using the correlation curves $C(t, \nu)$. Their presence on the correlation curves can only be noticed 1) from the deviation of the daily trend in the quiet Sun from the calculated one since compact sources do not produce such a trend and 2) from the reduction of the effect of convergence of the SRH correlation curves with an equidistant increase in frequency, which is typical of a homogeneous solar disk.

2.4. Radio bursts and satellites

Compact sources are best manifested in the structure of non-stationary events, which include radio bursts and the appearance of satellites in the SRH beam pattern. In this case, F_s=F_{burst} and C_s=C_{burst} (11). Here, F_{burst}=F–($F_\odot$+F_{AR}) is the radio flux increase in the burst; $F_\odot$+F_{AR} are the pre-burst values of the radio flux F; C_{burst}=C–($C_\odot$+C_{AR}) and $C_\odot$+C_{AR} are the pre-burst values of the points of the correlation curves C=$C(t, \nu)$. In the case of an ideal point source and in the absence of instrumental contributions, C_sF/F_s=1. The following product can therefore serve as an indicator of the compactness $\eta(\nu)$ of the microwave burst source

$$\eta(\nu) = C_{burst}F/F_{burst} \approx \frac{2J_1(\theta_{burst}/\theta_{beam})}{(\theta_{burst}/\theta_{beam})}. \tag{19}$$

The closer this ratio to unity, the more compact the radio source. The values $\theta_{burst}/\theta_{beam}$=1, 2, 3 correspond to $\eta(\nu)$≈0.88, 0.58, 0.23.

Geostationary satellites, unlike the distant Sun, rotate with Earth. The interferometer antennas track the Sun. Therefore, sometimes such satellites cross the beam pattern of single SRH antennas in. In this case, the situation is similar to that with a radio burst. The duration of such a radio burst, its profile and amplitude are determined by the rotation speed of Earth, the cross-section of the main and side lobes of the single-antenna beam pattern, and the power of the radio transmitter on the satellite. Geostationary satellites are located at an altitude of 36 thousand km from the Earth surface and, if they were observed at the zenith, this would be their minimum distance to SRH. The greatest altitude of the Sun above SRH is 61°. Geostationary satellites caught by the SRH beam pattern are, therefore, at a distance of at least 40000 km. As practically point radio sources, such satellites observed at frequencies <17 GHz are obviously located in the far wave field zone of SRH whose conditional boundary is $\simeq 2B_{max}^2/\lambda$, where B_{max} is the largest interferometer baseline. For these reasons, the equality $\eta(\nu) = 1$ should be satisfied for such satellites, which can be used as a condition for normalizing the values of $\eta(\nu)$ of solar radio bursts. Note that for satellites in medium and low orbits, the approximation of the far wave field of SRH is not fulfilled. There is a discrepancy between relations (10) and (11) obtained in this approximation and the instrumentally measured values of the correlation signal C_{burst}.

Thus, the spatial compactness of radio burst source $\eta(\nu)$ (19) can be estimated without analyzing two-dimensional images directly from the correlation curves $C(t, \nu)$ and the records of the total flux $F(t, \nu)$. The expected scatter of values of this parameter is considerably lower than that of other parameters associated with the radio burst, i.e. the radio flux, the soft X-ray and optical importance of the burst.

2.5. Secondary variations *C*(*t*, ν) of instrumental origin

The values of the points of the correlation curve C in (11) are functions of the spectral flux F, the set of κ_i SRH spatial harmonics, and the angular sizes of the emission sources θ so that $C = C\left(F, \theta, \kappa_i\right)$ (the mutual arrangement and diversity of shapes of radio sources are neglected). All these factors, in turn, are functions of time t and frequency ν. We are interested in the time derivative of the complex function $C(t, \nu)$:

$$\frac{\partial C}{\partial t} = C'_F \frac{\partial F}{\partial t} + C'_\theta \frac{\partial \theta}{\partial t} + \sum C'_{\kappa_i} \frac{\partial \kappa_i}{\partial t}, \tag{20}$$

where the apostrophe denotes the partial derivative of $C = C\left(F, \theta, \kappa_i\right)$. The situation with the quiet Sun when the first and second terms in this expression vanish was discussed in Section 2.1. In this case, the daily trend in the correlation curves $C_\odot$ with a minimum at noon is natural. However, against the background of the gradual daily trend, quasi-periodic variations are observed which are perceived as intensity variations of the emission flux. Such secondary variations are of purely instrumental origin and are caused by off-trend variations in the SRH beam pattern with unchanged angular size and emission flux of the radio source [Lesovoi, Kobets, 2018].

During a short radio burst, the changes in the beam pattern can be neglected by setting the third term in (20) equal to zero. If the size and shape of the burst source are constant, the variation $\delta C \propto \delta F$ during the burst is entirely due to the variation in its brightness temperature. During a radio burst, new emission centers often appear or the effective size of a single radio source (a rapidly lengthening arcade of flare loops) rapidly increases. The change in size can be taken into account by the assumed relation $F=F(\theta)$. Yet, the contribution of the second term in (20) to $C(t, \nu)$ will remain unaccounted.

The essence of the effect of variable angular size is known from the example with a two-antenna interferometer. The visibility of a radio source by one antenna pair is determined by only one term under the summation sign in (11). An increase in θ implies a quasi-periodic decrease in visibility, especially noticeable when the angular sizes of the source and spatial harmonic are comparable. The radioheliograph consists of a set of interferometers of different scales whose combined effect retouches the contribution of this effect to the correlation curve. Note that this contribution is practically imperceptible when all SRH antenna bases are employed. However, when selectively using, say, only correlations of high-frequency spatial harmonics for calculating correlation curves, such a contribution can lead to spurious pulsations C_{burst} with a fast frequency drift.

Thus, the quasi-periodic variations in the correlation response $C(t, \nu)$, which have no counterparts on the total-flux curves $F(t, \nu)$, are of instrumental origin.

2.6. Atmospheric absorption and correlation response

Observational experience has shown that intense precipitation and dense rain clouds cause a considerable decrease in the flux $F(\nu)$ of the received solar emission in almost the entire SRH frequency range. The decrease is due to the absorption and scattering of microwave emission by vapors and water droplets ([Alpert et al., 1953], [Stepanenko et al., 1987]). The contribution of microwave radiation absorption in Earth's atmosphere well exceeds the role of scattering, so it is sufficient to consider only absorption. One of the peaks of molecular absorption occurs at a frequency of 22 GHz. At about this frequency, the most significant decreases in the flux occur in SRH observations in rainy weather. For this reason, on rainy, snowy, and cloudy days, measurements of spectral fluxes of solar emission are prone to errors, sometimes quite large.

The correlation response is, in turn, much less susceptible to the influence of atmospheric absorption, as well as other factors of non-solar origin. In the idealized situation of the absence of intrinsic noise in the radioheliograph receiving system, such an influence simply does not exist. This statement follows from relations (11). Absorption and scattering equally reduce emission fluxes F, $F_\odot$, F_{AR}, and F_{burst}, which are in the numerator and denominator of these relations, and therefore the influence of absorption variations on the correlation response is compensated. In a real situation, the influence of external factors on the correlation response depends on the signal-to-noise ratio ([Lesovoi, Kobets, 2017]) and is especially pronounced under precipitation conditions, up to the disappearance of the SRH response to the recorded flux, and its correlation response.

Thus, the decrease in the solar radio flux $F(t, \nu)$, caused by atmospheric absorption, has a significant effect on the correlation response $C(t, \nu)$ only in relatively rare cases of intense precipitation.

CONCLUSION

The numerical value of each point on the correlation curve $C(t, \nu)$ is proportional to the sum of the amplitudes of the visibility functions $\boldsymbol{r}$ of all antenna pairs of the Siberian Radioheliograph. For this reason, the information potential of the curves $C(t, \nu)$ is in an intermediate position between the total-flux curves $F(t, \nu)$ and the sequence of two-dimensional images of the active Sun. The dependence of the correlation curves on the total flux, mutual arrangement, angular sizes and brightness of individual radio sources has its pros and cons.

The influence of the angular sizes of emission sources is the reason for the redistribution of the correlation response in favor of sources that are compact relative to the beam pattern $\theta_{beam}(t, \nu)$. For the same reason, the contribution of extended sources decreases. This redistribution determines 1) the high sensitivity of the correlation curves to weak and sufficiently compact sources and 2) a rapid decrease in the SRH correlation response to the quiet Sun with increasing frequency.

These circumstances, as well as the normalization division of the amplitudes of the visibility functions by the total flux in (8) and (11), prevent a correct assessment of spectral characteristics of a radio burst from the correlation plots. Variations in $\theta_{beam}(t, \nu)$ during the observation interval (day, year) determine variations and trend in the values of $C(t, \nu)$, which are not related to processes on the Sun.

Relations (11) can be used to estimate the contribution of the solar disk, active regions, and radio bursts to the SRH correlation curves. Of interest is the parameter of spatial compactness of radio burst source $\eta(\nu)$ (19), which can be easily estimated from the correlation curves $C(t, \nu)$ and the total-flux curves $F(t, \nu)$ without analyzing two-dimensional images. The maximum values of this parameter correspond to geostationary satellites.

Weather variations in atmospheric water content can cause significant variations in the solar radio flux $F(t, \nu)$. The correlation response $C(t, \nu)$ is much less susceptible to weather influence.

We are very grateful to the reviewers whose comments and suggestions improved the quality of the article.

The work was financially supported by the Ministry of Science and Higher Education of the Russian Federation. The Siberian Radioheliograph is a Unique Research Facility “Radioheliograph” [https://ckp-rf.ru/catalog/usu/4138190/].

REFERENCES

Alpert J.L., Ginzburg V.L., Feinberg E.L. *Rasprostranenie radiovoln* [Radio Wave Propagation]. Moscow, GITTL, 1953, 884 p. (In Russian).

Altyntsev A.T., Lesovoi S.V., Globa M.V., Gubin A.V., Kochanov A.A., Grechnev V.V., Ivanov E.F., et al. Multiwave Siberian Radioheliograph. *Solar-Terr. Phys*. 2020, vol. 6, iss. 2, pp. 30–40. DOI: 10.12737/stp62202003.

Borovik V.N. Quiet sun from multifrequency radio observations on RATAN-600. *Adv. Solar Phys*. 1994, vol. 432, pp. 185–190.

Fleishman G., Kontar E., Nita G., Gary D. *Cold, Tenuous Solar Flare: Acceleration Without Heating. Astrophys. J. Lett*. 2011, vol. 731, no. 1, pp. L19. DOI: 10.1088/2041-8205/731/1/L19.

Gradshtein I.S., Ryzhik I.M. Tables of Integrals, Series and Products. Moscow, Nauka, 1971, 1108 p. (In Russian).

Lesovoi S.V., Kobets V.S. Correlation plots of the Siberian Radioheliograph. *Solar-Terrestrial Physics*. 2017, vol. 3, iss. 1, pp. 19–25. DOI: 10.12737/article_58f96eeb8fa318.06122835.

Lesovoi S.V., Kobets V.S. Simulating Siberian Radioheliograph response to the quiet Sun. *Solar-Terrestrial Physics*. 2018, vol. 4, iss. 4, pp. 82–87. DOI: 10.12737/stp-44201811.

Stepanenko V.D., Shchukin G.G., Bobylev L.P., Matrosov S.Yu. *Radioteplolokatsiya v meteorologii* [Radiothermal Location in Meteorology]. Leningrad, Hydrometeoizdat, 1987, 280 p. (In Russian).

Thompson A.R., Moran J.M, Swenson G.W. Jr. Interferometry and Synthesis in Radio Astronomy. New York: Wiley, 2001. 692 p. DOI: 10.1002/9783527617845.

Nakajima H., Nishio M., Enome S., Shibasaki K., Takano T., Hanaoka, Y., Torii, C., et al. The Nobeyama radioheliograph. *IEEE Proc*. 1994, vol. 82, no. 5, pp. 705–713.

Yavorsky B.M., Detlaff A.A. *Spravochnik po fizike dlya inzhenerov i studentov vuzov* [Handbook of Physics For Engineers and University Students]. Moscow, Nauka, 1965. (In Russian).

Zheleznyakov V.V. Radio emission of the Sun and planets. International Series of Monographs in Natural Philosophy, Oxford: Pergamon Press. 1970.

Zirin H., Baumert B.M., Hurford G.J. The microwave brightness temperature spectrum of the quiet Sun. *Astrophys. J*. 1991, vol. 370, p. 779. DOI: 10.1086/169861.

Zlotnik E.Ya. Theory of the Slowly Changing Component of Solar Radio Emission.I. *Soviet Astronomy*. 1968, vol. 12, p. 245.

URL: https://www.swpc.noaa.gov/ (accessed August 12, 2024).

URL: https://badary.iszf.irk.ru/ (accessed August 12, 2024).

URL: https://ckp-rf.ru/catalog/usu/4138190/ (accessed August 12, 2024).

Original Russian version: Uralov A.M., Lesovoi S.V., Grechnev V.V., Globa M.V., published in Solnechno-zemnaya fizika. 2025, vol. 11, no. 1, pp. 88–97. DOI: 10.12737/szf-111202510.

How to cite this article

Uralov A.M., Lesovoi S.V., Grechnev V.V., Globa M.V. Features of correlation curves of the Siberian Radioheliograph. *Solar-Terrestrial Physics*. 2025, vol. 11, iss. 1, pp. 81–89. DOI: 10.12737/stp-111202510.